



Published in final edited form as:

Transl Stroke Res. 2011 December 1; 2(4): 619–632. doi:10.1007/s12975-011-0120-2.

Erythropoietin Mediates Neurobehavioral Recovery and Neurovascular Remodeling Following Traumatic Brain Injury in Rats by Increasing Expression of Vascular Endothelial Growth Factor

Ye Xiong, M.D., Ph.D.¹, Yanlu Zhang, M.D.¹, Asim Mahmood, M.D.¹, Yuling Meng, Ph.D.¹, Changsheng Qu, M.D.¹, and Michael Chopp, Ph.D.^{2,3}

¹Department of Neurosurgery, Henry Ford Health System, Detroit, MI, 48202

²Department of Neurology, Henry Ford Health System, Detroit, MI, 48202

³Department of Physics, Oakland University, Rochester, MI, 48309

Abstract

Erythropoietin (EPO) improves functional recovery after traumatic brain injury (TBI). Here, we investigated the role of vascular endothelial growth factor (VEGF) and VEGF receptor 2 (VEGFR2) on EPO-induced therapeutic efficacy in rats after TBI. Young male Wistar rats were subjected to unilateral controlled cortical impact injury and then infused intracerebroventricularly with either a potent selective VEGFR2 inhibitor SU5416 or vehicle dimethyl sulfoxide. Animals from both groups received delayed EPO treatment (5,000 U/kg in saline) administered intraperitoneally daily at 1, 2, and 3 days post injury. TBI rats treated with saline administered intraperitoneally daily at 1, 2, and 3 days post injury served as EPO treatment controls. 5-bromo-2-deoxyuridine was administered to label dividing cells. Spatial learning and sensorimotor function were assessed using a modified Morris water maze test and modified neurological severity score, respectively. Animals were sacrificed at 4 days post injury for measurement of VEGF and VEGFR2 or 35 days post injury for evaluation of cell proliferation, angiogenesis and neurogenesis. EPO treatment promoted sensorimotor and cognitive functional recovery after TBI. EPO treatment increased brain VEGF expression and phosphorylation of VEGFR2. EPO significantly increased cell proliferation, angiogenesis and neurogenesis in the dentate gyrus after TBI. Compared to the vehicle, SU5416 infusion significantly inhibited phosphorylation of VEGFR2, cell proliferation, angiogenesis, and neurogenesis as well as abolished functional recovery in EPO-treated TBI rats. These findings indicate the VEGF/VEGFR2 activation plays an important role in EPO-mediated neurobehavioral recovery and neurovascular remodeling after TBI.

Keywords

angiogenesis; erythropoietin; neurogenesis; traumatic brain injury; vascular endothelial growth factor

Introduction

Traumatic brain injury (TBI) is the leading cause of death and disability in young people [1]. The most prevalent and debilitating features in survivors of TBI are cognitive deficits and motor dysfunctions [2]. Despite advances in basic research as well as improved neurological intensive care in recent years, no effective pharmacological therapy for TBI is available that would promote functional recovery after TBI [3, 4]. Neurologic impairment is caused by both immediate brain tissue disruption (primary injury) and many postinjury cellular and molecular events (secondary injury) that worsen the primary neurologic insult. TBI clinical trials targeting a single pathophysiological pathway have failed; thus, it is likely that successful therapy may require targeting multiple injury pathways [3]. There is also an urgent need for efficient therapy to improve posttraumatic morbidity and mortality.

Erythropoietin (EPO) and the EPO receptor (EPOR), essential for erythropoiesis, are also expressed in neurons, astrocytes, and cerebral endothelial cells [5]. EPO is a multifunctional tissue protective agent with antiapoptotic, anti-inflammatory, antioxidative, angiogenic and neurotrophic properties [6, 7]. EPO is neuroprotective in animal models of stroke [8, 9], spinal cord injury [10], concussive brain injury [11], kainate-induced seizure activity [11], and autoimmune encephalomyelitis [12, 13]. Our recent work demonstrates that delayed treatment (24 h post injury) with EPO provides long-term benefits in rats after TBI [14, 15] and after stroke [8]. The therapeutic effects of the delayed administration of EPO are associated with increased angiogenesis and neurogenesis after TBI in rats [16–18]. However, mechanisms underlying EPO-induced angiogenesis and neurogenesis remain unclear after TBI. Here, we used a well-standardized experimental model of TBI in rats in combination with use of a potent selective VEGFR2 inhibitor SU5416 to determine the role of VEGF/VEGFR2 in EPO-mediated therapeutic effects after TBI, specifically, on neurobehavioral recovery and neurovascular remodeling.

Materials and Methods

All experimental procedures were approved by the Institutional Animal Care and Use Committee of Henry Ford Health System.

TBI Model

We used the controlled cortical impact (CCI) model of TBI in rat as previously described [19, 20]. Young adult male Wistar rats (344.5 ± 6.9 g) were anesthetized with an intraperitoneal injection of chloral hydrate (350 mg/kg body weight). Rectal temperature was maintained at 37°C using a feedback-regulated water-heating pad. A CCI device was used to induce injury. Rats were placed in a stereotactic frame. Two 10-mm-diameter craniotomies were performed adjacent to the central suture, midway between lambda and bregma. The second craniotomy allowed for lateral movement of cortical tissue. The dura mater was kept intact over the cortex. Injury was delivered by impacting the left (ipsilateral) cortex with a pneumatic piston containing a 6-mm-diameter tip at a rate of 4 m/s and 2.5 mm of compression. Velocity was measured with a linear velocity displacement transducer.

Experimental Groups and Treatment

TBI was induced in the rats by CCI over the left parietal cortex. The rats were divided into 4 groups ($n = 16$): 1) Sham; 2) Saline; 3) EPO + DMSO; and 4) EPO + SU5416. Sham rats underwent surgery without injury. EPO at a dose of 5,000 U/kg body weight (Epoetin alpha, AMGEN, Thousand Oaks, CA) was administered intraperitoneally at 24, 48 and 72 h after TBI. Animals in the saline-treated group received an equal volume of saline at 24, 48 and 72 h after TBI. For labeling proliferating cells, 5-bromo-2'-deoxyuridine (BrdU, 100 mg/kg;

Sigma) was injected intraperitoneally into rats daily for 10 days, starting 1 day after TBI. SU5416 is a potent selective inhibitor of the tyrosine kinase catalysis of VEGFR2 [21, 22]. To inhibit VEGFR2, animals were anesthetized intraperitoneally with chloral hydrate (350 mg/kg) and placed on a stereotactic apparatus (Harvard Apparatus, Holliston, MA). For infusion of SU5416 a cannula was placed into the right lateral ventricle (from the Bregma: anteroposterior, -0.8 mm; lateral, 1.5 mm; depth, 3.5 mm). The cannula was sealed with dental cement and connected to a 200 μ l, model 2002, Alzet pump (Alzet, Palo Alto, CA) with medical grade vinyl tubing. The minipump was implanted immediately after TBI in a subcutaneous pocket in the midscapular area of the back of the rat. The pumps were primed in a 37°C saline water bath overnight prior to insertion. Drug infusion was performed through the osmotic minipump filled with 4 mM SU5416 in 5% DMSO diluted in saline or vehicle at a rate of 0.5 μ l/h for 14 days. All rats were sacrificed at either 4 days for analysis of VEGF and VEGFR2 ($n = 4$) or 35 days after TBI for analysis of cell proliferation, angiogenesis and neurogenesis ($n = 8$).

Evaluation of Neurological Outcome

Morris Water Maze Test—All functional tests were performed by investigators blinded to the treatment status. To detect spatial learning, a recent version of the Morris water maze (MWM) test was used [23]. The procedure was modified from previous versions [24] and has been found to be useful for chronic spatial memory assessment in rats and mice with brain injury [15, 23]. Each rat received a block of four daily trials for five consecutive days (that is, 31–35 days post injury) to locate the hidden platform. The inter-trial interval was 30 min. Data collection was automated by the HVS Image 2020 Plus Tracking System (US HVS Image, San Diego, CA.). For data collection, a blue pool (1.8 m in diameter) was subdivided into four equal quadrants formed by imaging lines. At the start of a trial, the rat was placed at one of four fixed starting points, randomly facing toward a wall (designated North, South, East and West) and allowed to swim for 90 s or until it found the platform. If the animal found the platform, it was allowed to remain on it for 10 s. If the animal failed to find the platform within 90 s, it was placed on the platform for 10 s. Throughout the test period the platform was located in the Northeast quadrant 2 cm below water in a randomly changing position, including locations against the wall, toward the middle of the pool or off-center but always within the target quadrant. If the animal was unable to find the platform within 90 s, the trial was terminated and a maximum score of 90 s was assigned. If the animal reached the platform within 90 s, the percentage of time traveled within the Northeast (correct) quadrant was calculated relative to the total amount of time spent swimming before reaching the platform and employed for statistical analysis. The advantage of this version of the water maze is that each trial takes on the key characteristics of a probe trial because the hidden platform is not in a fixed location within the target quadrant [25]. This method allows animals to probe spatial memory early and continuously as the animals learn. In addition, the animals are unlikely to adopt an intermediate strategy of looping around the tank at a specific distance away from the wall, a response that gets them to a fixed platform quite rapidly without the use of distal visual cues, and which does not require the hippocampus [25].

Modified Neurological Severity Score (mNSS) Test—Neurological functional measurement was performed using the mNSS score [26]. The test was carried out on all rats preinjury and on days 1, 4, 7, 14, 21, 28, and 35 after TBI. The mNSS score is a composite of the motor (muscle status, abnormal movement), sensory (visual, tactile and proprioceptive) and reflex tests and has been employed in previous studies [27]. This test is suitable for evaluating long-term neurological function after unilateral brain injury [18].

Tissue Preparation and Measurement of Lesion Volume

On day 35 after TBI, rats were anesthetized intraperitoneally with chloral hydrate and perfused transcardially first with saline solution, followed by 4% paraformaldehyde in 0.1 M PBS (pH 7.4). Brains were removed and post-fixed in 4% paraformaldehyde for 2 days at room temperature. The brain tissue was cut into 7 equally spaced 2-mm coronal blocks and processed for paraffin sectioning. A series of adjacent 6- μ m-thick sections were cut from each block in the coronal plane and stained with hematoxylin and eosin (H & E). For lesion volume measurement, the 7 brain sections were traced by a microcomputer imaging device (MCID) (Imaging Research, St. Catharines, Ontario, Canada), as previously described [28, 29]. The lesion volume was presented as a volume percentage of the lesion compared with the contralateral hemisphere.

Immunohistochemistry

To examine the effect of EPO on cell proliferation and angiogenesis, coronal sections were immunohistochemically stained with the mouse anti-BrdU and the mouse anti-endothelial barrier antigen (EBA) antibody, respectively. Briefly, 6- μ m paraffin-embedded coronal sections were deparaffinized and rehydrated. Antigen retrieval was performed by boiling sections in 10-mM citrate buffer (pH 6.0) for 10 min. After washing with PBS, sections were incubated with 0.3 % H₂O₂ in PBS for 10 min, blocked with 1% BSA containing 0.3 % Triton-X 100 for 1 h at room temperature, and incubated with mouse anti-BrdU antibody (1:200; Dako, Carpinteria, CA) at 4°C overnight. After washing, sections were incubated with biotinylated anti-mouse antibody (1:200; Vector Laboratories, Inc., Burlingame, CA) for 30 min at room temperature. After an additional washing, sections were incubated with an avidin-biotin-peroxidase system (ABC kit, Vector Laboratories, Inc.). Diaminobenzidine (Sigma, St. Louis, MO) was then used as a sensitive chromogen for light microscopy. Sections were counterstained with hematoxylin.

To identify vascular structure, brain sections were deparaffinized and then incubated with 0.4% Pepsin solution at 37°C for 1 h. After washing, the sections were blocked with 1% BSA at room temperature for 1 h, and then incubated with mouse anti-EBA antibody (SMI-71, 1:1000, Covance, Berkeley, CA) at 4°C overnight. The subsequent procedures were the same as for BrdU staining. BrdU-positive cells and EBA-stained vessels in the dentate gyrus and the cortex of ipsilateral hemispheres were examined at X20 magnification and counted [15].

Immunofluorescent Staining

Newly generated neurons were identified by double labeling for BrdU and NeuN. After dehydration, coronal sections were boiled in 10 mM citric acid buffer (pH 6) for 10 min. Sections were incubated in 2.4 N HCl at 37°C for 20 min. Sections were incubated with 1% BSA containing 0.3% Triton-X-100 in PBS, and then incubated with mouse anti-NeuN antibody (1:200; Chemicon) at 4°C overnight. After incubation with FITC-conjugated anti-mouse antibody (1:400; Jackson ImmunoResearch) at room temperature for 2 h, sections were incubated with rat anti-BrdU antibody (1:200; Dako) at 4°C overnight. Sections were then incubated with Cy3-conjugated anti-rat antibody (1:400; Jackson ImmunoResearch) at room temperature for 2 h. Coronal sections were mounted with Vectashield mounting medium (Vector Laboratories).

Our previous study showed that VEGF expression is increased in the astrocytes after TBI and treatment [30]. To examine the effect of EPO and SU5416 treatment on expression of VEGF in astrocytes after TBI, a polyclonal IgG anti-VEGF antibody (Santa Cruz Biotechnology, Santa Cruz, CA) at a titer of 1: 400 was used to incubate the brain sections at 4°C overnight. The secondary antibody (Cy3, 1:200 in PBS, Jackson ImmunoResearch,

West Grove, PA) followed. Each of the aforementioned steps was followed by four 5-min rinses in PBS. Rabbit anti-gial fibrillary acidic protein (GFAP) was used to detect astrocytes in injured brain. The second antibody (FITC, 1:200 in PBS, Jackson ImmunoResearch) was added at room temperature for 30 min. The sections were counterstained with 4', 6-diamidino-2-phenyl-indole, dihydrochloride for the identification of nuclei.

Cell Counting and Quantitation

The methods we used here to count cells have been widely utilized in our previous studies [31–34]. We did not employ stereological counting methods but we counted cells using the principles of stereology [32]. This method permits a meaningful comparison of differences among groups. For quantitative measurements of cells, five sections from each brain were employed with the epicenter of the injury cavity at bregma -3.3 mm and 100- μ m intervals between adjacent sections. Images were taken from each section containing eight fields of view in the lesion boundary zone, three fields of view in the ipsilateral CA3 and CA1, and nine fields of view in the ipsilateral dentate gyrus. The fields were digitized and analyzed with a Nikon i80 microscope at a magnification of 200 or 400 via the MCID system [15]. All counting was performed on a computer monitor to improve visualization and in one focal plane to avoid oversampling [35]. To evaluate whether EPO administered intraperitoneally reduces neuronal damage after TBI, the number of cells was counted in the hippocampus. Although H&E staining is not neuron-specific, the morphological characteristics of neuronal cells in the dentate gyrus, CA1, and CA3 region aid in counting them. Counts were averaged and normalized by measuring the linear distance (in mm) of the dentate gyrus, CA1 and CA3 for each section. Although it is just an estimate of the cell number, this method permits a meaningful comparison of differences between groups [16–18]. For cell proliferation, the total number of BrdU-positive cells was counted in the lesion boundary zone and the dentate gyrus. The cells with BrdU (brown stained) that clearly localized to the nucleus (hematoxylin stained) were counted as BrdU-positive cells. The number of BrdU-positive cells was expressed in cells/mm². To evaluate neurogenesis, BrdU/NeuN-labeled cells were counted in the dentate gyrus. The number of GFAP/VEGF-labeled cells was counted in the cortex (lesion boundary zone) and hippocampus.

Western Blot Analysis

Rats were sacrificed at 4 days after TBI (4 per group). Brain tissues from the lesion boundary zone and the hippocampus were collected, washed once in PBS, and lysed in lysis buffer (20 mM Tris pH 7.6, 100 mM NaCl, 1% Nonidet P-40, 0.1% SDS, 1% deoxycholic acid, 10% glycerol, 1 mM EDTA, 1 mM NaVO₃, 50 mM NaF, cocktail I of protease inhibitors from Calbiochem, Gibbstown, NJ). After sonication, soluble protein was obtained by centrifugation at 13,000 $\times g$ for 15 min at 4°C. The protein concentration of each sample was determined by bicinchoninic acid (BCA) protein assay (Pierce, Rockford, IL). For immunoblotting equal amounts of cell lysate were subjected to electrophoresis on 10% or 14% SDS-polyacrylamide gels. Separated proteins were then electrotransferred to Immobilon membranes (Millipore, Bedford, MA). Membranes were blocked in 2% I-Block powder (Tropix, Redford, MA) in PBS plus 0.1% Tween-20 at room temperature and then incubated with different primary antibodies at 4°C overnight. The following antibodies were used: VEGF and VEGFR2 (1:1000; Cell Signaling Technology, Beverly, MA), anti-p-VEGFR2 (1:1000; Millipore) and anti-Actin (1:1000; Santa Cruz Biotechnology). After washing with TBS-T, membranes were incubated with HRP-conjugated secondary antibodies (1:2500; Jackson Immunological Research Laboratory) in blocking solution at room temperature for 2 h. Proteins were visualized by using an enhanced chemiluminescence protein detection kit (Pierce). Membranes were subsequently stripped with stripping buffer (Pierce) for 30 min at room temperature, washed extensively with

TBS-T, blocked, and then reprobed as described above. The intensity of the bands was measured using Scion image analysis (Scion Corporation, Frederick, MD).

Statistical Analyses

All data are presented as mean plus \pm SD. Data on mNSS were first evaluated for normality. The rank data were used for the analysis since mNSS data were not normal. Analyses of variance (ANOVA) and PROC MIXED with CONTRAST statement in SAS, were employed to test the group difference on mNSS. The analysis began testing the overall group effect. If overall group effect was detected at the 0.05 level, then pair-wise group comparisons were performed; otherwise pair-wise group comparisons were considered as exploratory analyses. Data on spatial learning function were analyzed by ANOVA for repeated measurements. For lesion volume, cell counting, EBA-stained vascular density, and Western blot data, a one-way ANOVA followed by post hoc Student-Newman-Keuls test was used to compare the differences between the sham-, saline-, EPO+DMSO-, and EPO+SU5416-treated groups. Pearson's correlation coefficients were calculated between the histological outcomes and the behavioral scores. Statistical significance was set at $P < 0.05$.

Results

Spatial Learning Test

To analyze day-by-day differences in the MWM, a repeated-measures ANOVA was performed and followed by Student-Newman-Keuls tests for multiple comparisons. As shown in Figure 1a, the percentage of time spent in the correct quadrant (northeast) by sham rats gradually increased from days 31 to 35 after surgery. The greater the percentage of time spent in the correct quadrant, the better the spatial learning. The spatial learning of the saline-treated rats with TBI was significantly impaired compared to sham-operated rats at days 32–35 ($P < 0.05$) after injury. As compared to saline treatment, EPO+DMSO-treated rats with TBI showed significant improvement at day 32–35 ($P < 0.05$). However, as compared to the EPO+DMSO group, the EPO+SU5416 group showed significant deficits in spatial learning (a smaller percentage of time spent in the correct quadrant) at day 32–35 ($P < 0.05$). Moreover, spatial learning function in the EPO+SU5416 group was worse than that in the saline group at day 35 compared to saline treatment ($P < 0.05$).

Neurological Severity Score

Figure 2b shows that there is no significant difference in the mNSS among the saline-, EPO + DMSO-, and EPO + SU5416-treated groups at day 1 post TBI, indicating that the severity of injury among these groups was comparable. TBI significantly increased the mNSS (the higher the mNSS, the worse the sensorimotor function) at 1 to 35 days post injury compared to the sham groups ($P < 0.05$ for days 1 to 35). However, significantly reduced scores were measured at days 4 to 35 after TBI in the EPO+DMSO-treated group compared to the saline-treated group ($P < 0.05$). The EPO+SU5416 group showed significantly less functional recovery at days 4–35 compared to the EPO+DMSO treatment ($P < 0.05$). Moreover, the EPO+SU5416 group had a significantly higher mNSS at day 35 compared to the saline-treated group ($P < 0.05$).

Lesion Volume

Lesion volume measurements were performed at 35 days post TBI. In the present study, TBI caused consistent cortical lesion (Fig. 2). The EPO+DMSO group exhibited a trend to reduce the lesion volume but lesion volumes were not significantly different from the saline-treated group (Fig. 2, $P > 0.05$). The EPO+SU5416 group showed a trend to increase the

lesion volume, but lesion volume was not significantly different from the saline-treated group ($P>0.05$).

Cell Loss in the Hippocampus

When examined at 35 days post TBI (Fig. 3), the neuron counts in the CA3, dentate gyrus, and CA1 of the ipsilateral hippocampus decreased significantly after TBI (Fig. 3b, f and h, $P<0.05$) compared to sham controls (Fig. 3a and e). As compared to saline controls, the EPO +DMSO- treated group showed significantly increased neuron counts in these regions (Fig. 3c, g, and i, $P<0.05$), while the EPO+SU5416-treated group showed significantly decreased neuron counts in these regions as compared to the EPO+DMSO-treated group (Fig. 3d, h, and i; $P<0.05$). The neurons counts in the EPO+SU5416-treated group were comparable to those in the saline-treated group.

Angiogenesis

EBA is a specific immunohistochemical marker of central nervous system microvessels which has been used to quantitatively assess microvascular alterations following TBI [36] and stroke [37, 38]. TBI alone significantly increased the vascular density in the cortex, dentate gyrus, and CA3 of the ipsilateral hemisphere (Fig. 4b, f, and j, $P<0.05$) at 35 days after TBI compared to sham controls (Fig. 4a, e, and i). EPO+DMSO treatment significantly increased the vascular density in the cortex, dentate gyrus and CA3 (Fig. 4c, g, and k, $P<0.05$) compared to saline treatment. Treatment with EPO+SU5416 (Fig. 4d, h, and i) significantly reduced vascular density in these regions compared to treatment with EPO +DMSO (Fig. 4c, g, and k, $P<0.05$). In addition, treatment with EPO+SU5416 significantly reduced vascular density in these regions compared to treatment with saline (Fig. 4b, f, and j, $P<0.05$).

Cell Proliferation

BrdU labeling is commonly used to detect cell proliferation [15]. The number of BrdU-positive cells found in the ipsilateral cortex and dentate gyrus (Fig. 5b and f, $P<0.05$) was significantly increased at 35 days after TBI, compared with sham controls (Fig. 5a and e). However, EPO+DMSO treatment further increased the number of BrdU-positive cells in the cortex and dentate gyrus (Fig. 5c and g, $P<0.05$) after TBI compared to saline controls. A significantly lower density of BrdU-positive cells in these regions was observed in the EPO +SU5416 group compared to the EPO+DMSO group (Fig. 5d and h, $P<0.05$). Moreover, the EPO+SU5416-treated group showed significantly reduced cell proliferation in these regions compared to the saline-treated group (Fig. 4b, f, and i, $P<0.05$).

Neurogenesis

Newly generated neurons were identified by double staining for BrdU (proliferating marker) and NeuN (mature neuronal marker). The number of NeuN/BrdU-colabeled cells (newborn neurons) was significantly higher in the ipsilateral dentate gyrus of the saline-treated group (Fig. 6b and e, $P<0.05$) at 35 days after TBI compared to sham controls (Fig. 6a). The number of newborn neurons was significantly increased in the ipsilateral dentate gyrus of the EPO+DMSO-treated group (Fig. 6c and e, $P<0.05$) compared to the saline-treated group. In addition, the number of newborn neurons in the injured dentate gyrus was significantly lower in the EPO+SU5416-treated group than in the EPO+DMSO-treated group (Fig. 6d and e, $P<0.05$). TBI significantly reduced the percentage of newly generated cells in the DG that differentiate into mature neurons in the saline group as compared to sham controls (Fig. 6f, $P<0.05$). EPO+DMSO treatment increased the number of newly generated cells that differentiate into mature neurons to a level comparable to that seen in sham controls. The percentage of newborn neurons in the EPO+SU5416-treated group was significantly reduced

compared to the EPO+DMSO-treated group ($P<0.05$). In addition, both the number of newborn neurons and the percentage of the newly generated cells to differentiate into mature neurons in these regions were significantly reduced in the EPO+SU5416-treated group compared to that seen in the saline-treated group (Fig. 6b, d, e, and f, $P<0.05$).

Correlation of Histological Changes with Functional Recovery

Data from all four groups were included to generate the correlations between functional and histological outcomes. This correlation analysis has been widely used to correlate behavior with histological outcomes in stroke and TBI studies [33, 39–42]. Correlation analyses indicate that sensorimotor functional deficits (as measured by mNSS at 35 days after TBI) are highly and positively correlated to cortical lesion size (Fig. 7a), and inversely correlated to the vascular density in the injured cortex (Fig. 7b) examined at day 35 after TBI ($P<0.05$). Spatial learning at 35 days after TBI (percentage of time spent in correct quadrant) is highly and positively correlated to neuron counts (Fig. 7c) and vascular density in the injured dentate gyrus, CA3, and CA1 (Fig. 7d) as well as to the number of newborn neurons in the dentate gyrus (Fig. 7e) assessed at day 35 after TBI ($P<0.05$). These data indicate that delayed EPO therapy improves neurological recovery most likely by reducing neuronal loss and promoting angiogenesis and neurogenesis.

EPO Increases VEGF Expression and p-VEGFR2 in the Injured Brain

Western blot analysis revealed that VEGF and p-VEGFR2 level increased in the injury boundary zone and hippocampus at 4 days after TBI (Fig.8, $P<0.05$). Delayed EPO treatment significantly increased VEGF level and phosphorylation of VEGFR2. SU5416 infusion did not significantly affect brain VEGF level and expression of VEGFR2 but significantly reduced phosphorylation of VEGFR2.

EPO Increases VEGF Expression in the Astrocytes

The expression of VEGF in astrocytes was detected with triple staining (VEGF, GFAP and DAPI, Fig.9). Triple staining showed that more astrocytes in the boundary zone and hippocampus were VEGF-positive in the EPO+DMSO-treated group compared to the saline-treated group ($P<0.05$). SU5416 infusion did not affect VEGF expression in the astrocytes compared to the EPO+DMSO-treated group ($P<0.05$).

Discussion

In this study, we demonstrate that: 1) EPO treatment increases brain VEGF expression and phosphorylation of VEGFR2 after TBI; 2) the EPO-mediated sensorimotor and cognitive functional recovery are highly and significantly correlated to increased cell proliferation, angiogenesis and neurogenesis; and 3) inhibition of VEGFR2 by SU5416 significantly decreases cell proliferation, angiogenesis and neurogenesis as well as abolishes the EPO-mediated sensorimotor and cognitive functional recovery after TBI in rats. These findings indicate that VEGF/VEGFR2 activation at least partially contributes to EPO treatment-mediated neurobehavioral recovery and neurovascular remodeling after TBI.

Our previous study demonstrates that mice with EPO receptor null in the nervous system exhibit aggravated sensorimotor deficits after TBI [43]. Using knockout techniques, Tsai et al. provide strong evidence that endogenous EPO and the classical EPOR play a critical role in nervous system development and adult brain repair after stroke [44]. These results indicate that endogenous EPO contributes to spontaneous recovery processes after brain injury. Neuroprotection by EPO has usually been observed when EPO is administered within 6 h after brain injury [11, 45–47]. Our recent findings demonstrate that delayed (24-h post injury) repeated EPO therapy does not reduce cortical lesion volume but improves

functional outcomes after TBI and stroke [8, 15, 18], indicating that the therapeutic window of EPO may not be limited to the early hours after acute brain injury. Furthermore, our previous study suggests that EPO-induced therapeutic effects on TBI rats are independent of EPO-stimulated hematopoietic effects [48] but highly dependent on reducing hippocampal neuron loss, and increasing angiogenesis and neurogenesis in a dose-dependent manner [16]. The mechanisms underlying the EPO therapeutic effects have not been fully investigated. It is widely accepted that EPO's neuroprotective mechanisms are related to EPOR binding [49]. However, there is evidence that the hematopoietic effect and tissue protection may act through different receptors [50]. For example, carbamylated EPO (CEPO) or certain EPO mutants do not bind to the classical EPOR and do not show any hematopoietic activity in human cell signaling assays or on chronic dosing in different animal species [50]. However, CEPO and various nonhematopoietic mutants confer neuroprotection at a potency and efficacy comparable to EPO [14, 50–53]. It is believed that EPOR and beta common receptor comprise a tissue-protective heteroreceptor because neither EPO nor CEPO was active in cardiomyocyte or spinal cord injury models performed in the beta common receptor knockout mouse [54].

Studies from us and others demonstrate that VEGF/VEGFR expression is upregulated in TBI animals [30, 55–57]. In addition, inhibition by VEGFR2 antagonists increases lesion size and cellular death, decreases neurogenesis, and exacerbates functional impairments after TBI [58–61]. These findings suggest that increased endogenous expression of VEGF and VEGFR2 after TBI is favorable for spontaneous functional outcome. Furthermore, intracerebroventricular infusion of VEGF significantly augments neurogenesis and angiogenesis, reduces lesion volumes and improves functional outcome in mice after TBI [62]. Our prior studies demonstrate that delayed EPO treatment initiated 24 h post injury improves functional recovery after TBI [16–18, 43, 48]. Whether delayed EPO treatment-mediated functional recovery, angiogenesis and neurogenesis after TBI are associated with upregulation of VEGF/VEGFR2 signaling pathway has not been investigated. In the present study, Western blot data clearly show that EPO treatment (without SU5416 infusion) significantly increases expression of VEGF and phosphorylation of VEGFR2 and improves functional recovery after TBI. The number of VEGF-positive astrocytes is significantly greater in the brain of the EPO-treated TBI rat compared to the saline-treated TBI rat. These new findings indicate that delayed EPO treatment-mediated functional improvement is at least partially associated with increased expression of VEGF in the astrocytes. To further verify the role of EPO-mediated upregulation of VEGF/VEGFR2 signaling pathway in functional recovery, we performed an additional experiment in EPO-treated TBI rats with inhibition of VEGFR2 by SU5416. SU5416 infusion did not change the VEGF level but effectively and significantly decreased phosphorylation of VEGFR2 as well as abolished functional recovery in EPO-treated TBI rats. Collectively, these data indicate that upregulation of the VEGF/VEGFR2 signaling pathway plays an important role in EPO-mediated functional improvement after TBI.

The adult brain vascular system is stable under normal conditions, but is activated in response to certain pathological conditions including injuries [63]. Our previous study shows that EPO promotes angiogenesis after TBI in a dose-dependent manner [16]. The coupling of angiogenesis and neurogenesis has been demonstrated in rodents after brain injuries [8, 64–66]. Angiogenesis may provide the critical neurovascular microenvironment for neuronal remodeling [63, 67–71]. Treatment with EPO contributes to neurovascular remodeling, leading to improved neurobehavioral outcomes following ischemic brain injury [8, 72]. How EPO induces angiogenesis after TBI is unclear. Our in vitro study shows that EPO enhances VEGF secretion in neural progenitor cells through activation of the PI3K/Akt and ERK1/2 signal-transduction pathways and that neural progenitor cells treated with EPO upregulate VEGFR2 expression in cerebral endothelial cells, which along with VEGF

secreted by neural progenitor cells promotes angiogenesis [73]. Our present study shows that EPO treatment increases VEGF expression in astrocytes and inhibition of VEGFR2 abolishes angiogenesis as well as functional recovery after TBI. These data collectively suggest that VEGF/VEGFR2 plays an important role in EPO-mediated angiogenesis after TBI.

Increasing evidence shows that EPO not only stimulates vascular repair but also promotes neurogenesis after brain injury [7, 8, 16–18, 73, 74]. EPO enhances neurogenesis in animal models of TBI [15–18] and stroke [8, 9, 44]. VEGF may play an important role in EPO-mediated neurogenesis after TBI. In addition to its robust angiogenic effects, VEGF is capable of promoting neurogenesis in response to TBI [61, 62]. In the present study, inhibition of VEGFR2 not only reduced EBA-labeled vascular density (an index of angiogenesis) but also reduced the number of newborn neurons in the dentate gyrus in EPO-treated TBI rats. Furthermore, SU5416 decreased the percentage of newly generated (BrdU-positive) cells to differentiate into mature neurons (BrdU/NeuN colabeled cells) in EPO-treated TBI rats. These data indicate that VEGFR2 activation participates in EPO-mediated neurovascular remodeling after TBI. SU5416 is a potent selective inhibitor of the tyrosine kinase catalysis of VEGFR2 and is used for inhibition of VEGFR2 in TBI research [21, 22, 59–61]. However, SU5416 also inhibits other tyrosine kinases including VEGFR1 [75]. The present study cannot rule out that other angiogenic factors and their receptors may also be involved in the EPO therapeutic effects. Further studies are warranted.

In conclusion, to the best of our knowledge, this study is the first to examine the role of VEGF/VEGFR2 in the EPO-mediated therapeutic effects after TBI in rats, specifically EPO-improved neurobehavioral recovery and neurovascular remodeling. Although the causal link between behavior and histological outcomes after TBI and EPO treatment has not been established, the correlation analysis shows that there is a significant association between them. These data extend our knowledge on mechanisms underlying delayed EPO treatment-mediated therapeutic efficacy after TBI.

Acknowledgments

This work was supported by NIH grants RO1 NS62002 to Y. Xiong and PO1 NS023393 to M. Chopp. Special thanks to Ms. Susan MacPhee-Gray for editorial assistance.

References

1. Beauchamp K, Mutlak H, Smith WR, Shohami E, Stahel PF. Pharmacology of traumatic brain injury: where is the "golden bullet"? *Mol Med*. 2008; 14(11–12):731–740. [PubMed: 18769636]
2. Davis AE. Mechanisms of traumatic brain injury: biomechanical, structural and cellular considerations. *Crit Care Nurs Q*. 2000; 23(3):1–13. [PubMed: 11852934]
3. Narayan RK, Michel ME, Ansell B, Baethmann A, Biegon A, Bracken MB, Bullock MR, Choi SC, Clifton GL, Contant CF, Coplin WM, Dietrich WD, Ghajar J, Grady SM, Grossman RG, Hall ED, Heetderks W, Hovda DA, Jallo J, Katz RL, Knoller N, Kochanek PM, Maas AI, Majde J, Marion DW, Marmarou A, Marshall LF, McIntosh TK, Miller E, Mohberg N, Muizelaar JP, Pitts LH, Quinn P, Riesenfeld G, Robertson CS, Strauss KI, Teasdale G, Temkin N, Tuma R, Wade C, Walker MD, Weinrich M, Whyte J, Wilberger J, Young AB, Yurkewicz L. Clinical trials in head injury. *J Neurotrauma*. 2002; 19(5):503–557. [PubMed: 12042091]
4. Royo NC, Schouten JW, Fulp CT, Shimizu S, Marklund N, Graham DI, McIntosh TK. From cell death to neuronal regeneration: building a new brain after traumatic brain injury. *J Neuropathol Exp Neurol*. 2003; 62(8):801–811. [PubMed: 14503636]
5. Noguchi CT, Wang L, Rogers HM, Teng R, Jia Y. Survival and proliferative roles of erythropoietin beyond the erythroid lineage. *Expert Rev Mol Med*. 2008; 10:e36. [PubMed: 19040789]

6. Cotena S, Piazza O, Tufano R. The use of erythropoietin in cerebral diseases. *Panminerva Med.* 2008; 50(2):185–192. [PubMed: 18607342]
7. Velly L, Pellegrini L, Guillet B, Bruder N, Pisano P. Erythropoietin 2nd cerebral protection after acute injuries: a double-edged sword? *Pharmacol Ther.* 2010; 128(3):445–459. [PubMed: 20732352]
8. Wang L, Zhang Z, Wang Y, Zhang R, Chopp M. Treatment of stroke with erythropoietin enhances neurogenesis and angiogenesis and improves neurological function in rats. *Stroke.* 2004; 35(7): 1732–1737. [PubMed: 15178821]
9. Gonzalez FF, McQuillen P, Mu D, Chang Y, Wendland M, Vexler Z, Ferriero DM. Erythropoietin enhances long-term neuroprotection and neurogenesis in neonatal stroke. *Dev Neurosci.* 2007; 29(4–5):321–330. [PubMed: 17762200]
10. Grasso G, Sfacteria A, Erbayraktar S, Passalacqua M, Meli F, Gokmen N, Yilmaz O, La Torre D, Buemi M, Iacopino DG, Coleman T, Cerami A, Brines M, Tomasello F. Amelioration of spinal cord compressive injury by pharmacological preconditioning with erythropoietin and a nonerythropoietic erythropoietin derivative. *J Neurosurg Spine.* 2006; 4(4):310–318. [PubMed: 16619678]
11. Brines ML, Ghezzi P, Keenan S, Agnello D, de Lanerolle NC, Cerami C, Itri LM, Cerami A. Erythropoietin crosses the blood-brain barrier to protect against experimental brain injury. *Proc Natl Acad Sci U S A.* 2000; 97(19):10526–10531. [PubMed: 10984541]
12. Sakanaka M, Wen TC, Matsuda S, Masuda S, Morishita E, Nagao M, Sasaki R. In vivo evidence that erythropoietin protects neurons from ischemic damage. *Proc Natl Acad Sci U S A.* 1998; 95(8):4635–4640. [PubMed: 9539790]
13. Cerami A. Beyond erythropoiesis: novel applications for recombinant human erythropoietin. *Semin Hematol.* 2001; 38 Suppl 7(3):33–39. [PubMed: 11523026]
14. Mahmood A, Lu D, Qu C, Goussev A, Zhang ZG, Lu C, Chopp M. Treatment of traumatic brain injury in rats with erythropoietin and carbamylated erythropoietin. *J Neurosurg.* 2007; 107(2):392–397. [PubMed: 17695395]
15. Lu D, Mahmood A, Qu C, Goussev A, Schallert T, Chopp M. Erythropoietin enhances neurogenesis and restores spatial memory in rats after traumatic brain injury. *J Neurotrauma.* 2005; 22(9):1011–1017. [PubMed: 16156716]
16. Meng Y, Xiong Y, Mahmood A, Zhang Y, Qu C, Chopp M. Dose-dependent neurorestorative effects of delayed treatment of traumatic brain injury with recombinant human erythropoietin in rats. *J Neurosurg.* 2011
17. Ning R, Xiong Y, Mahmood A, Zhang Y, Meng Y, Qu C, Chopp M. Erythropoietin promotes neurovascular remodeling and long-term functional recovery in rats following traumatic brain injury. *Brain Res.* 2011; 1384:140–150. [PubMed: 21295557]
18. Xiong Y, Mahmood A, Meng Y, Zhang Y, Qu C, Schallert T, Chopp M. Delayed administration of erythropoietin reducing hippocampal cell loss, enhancing angiogenesis and neurogenesis, and improving functional outcome following traumatic brain injury in rats: comparison of treatment with single and triple dose. *J Neurosurg.* 2010; 113(3):598–608. [PubMed: 19817538]
19. Dixon CE, Clifton GL, Lighthall JW, Yaghami AA, Hayes RL. A controlled cortical impact model of traumatic brain injury in the rat. *J Neurosci Methods.* 1991; 39(3):253–262. [PubMed: 1787745]
20. Mahmood A, Lu D, Chopp M. Marrow stromal cell transplantation after traumatic brain injury promotes cellular proliferation within the brain. *Neurosurgery.* 2004; 55(5):1185–1193. [PubMed: 15509325]
21. Fong TA, Shawver LK, Sun L, Tang C, App H, Powell TJ, Kim YH, Schreck R, Wang X, Risau W, Ullrich A, Hirth KP, McMahon G. SU5416 is a potent and selective inhibitor of the vascular endothelial growth factor receptor (Flk-1/KDR) that inhibits tyrosine kinase catalysis, tumor vascularization, and growth of multiple tumor types. *Cancer Res.* 1999; 59(1):99–106. [PubMed: 9892193]
22. Mendel DB, Schreck RE, West DC, Li G, Strawn LM, Tanciongco SS, Vasile S, Shawver LK, Cherrington JM. The angiogenesis inhibitor SU5416 has long-lasting effects on vascular endothelial growth factor receptor phosphorylation and function. *Clin Cancer Res.* 2000; 6(12): 4848–4858. [PubMed: 11156244]

23. Choi SH, Woodlee MT, Hong JJ, Schallert T. A simple modification of the water maze test to enhance daily detection of spatial memory in rats and mice. *J Neurosci Methods*. 2006; 156(1–2): 182–193. [PubMed: 16621016]
24. Morris R. Developments of a water-maze procedure for studying spatial learning in the rat. *J Neurosci Methods*. 1984; 11(1):47–60. [PubMed: 6471907]
25. Schallert T. Behavioral tests for preclinical intervention assessment. *NeuroRx*. 2006; 3(4):497–504. [PubMed: 17012064]
26. Chen J, Sanberg PR, Li Y, Wang L, Lu M, Willing AE, Sanchez-Ramos J, Chopp M. Intravenous administration of human umbilical cord blood reduces behavioral deficits after stroke in rats. *Stroke*. 2001; 32(11):2682–2688. [PubMed: 11692034]
27. Lu D, Mahmood A, Qu C, Hong X, Kaplan D, Chopp M. Collagen scaffolds populated with human marrow stromal cells reduce lesion volume and improve functional outcome after traumatic brain injury. *Neurosurgery*. 2007; 61(3):596–602. discussion 602-593. [PubMed: 17881974]
28. Chen J, Zhang C, Jiang H, Li Y, Zhang L, Robin A, Katakowski M, Lu M, Chopp M. Atorvastatin induction of VEGF and BDNF promotes brain plasticity after stroke in mice. *J Cereb Blood Flow Metab*. 2005; 25(2):281–290. [PubMed: 15678129]
29. Swanson RA, Morton MT, Tsao-Wu G, Savalos RA, Davidson C, Sharp FR. A semiautomated method for measuring brain infarct volume. *J Cereb Blood Flow Metab*. 1990; 10(2):290–293. [PubMed: 1689322]
30. Qu C, Mahmood A, Liu XS, Xiong Y, Wang L, Wu H, Li B, Zhang ZG, Kaplan DL, Chopp M. The treatment of TBI with human marrow stromal cells impregnated into collagen scaffold: functional outcome and gene expression profile. *Brain Res*. 2011; 1371:129–139. [PubMed: 21062621]
31. Chen J, Li Y, Zhang R, Katakowski M, Gautam SC, Xu Y, Lu M, Zhang Z, Chopp M. Combination therapy of stroke in rats with a nitric oxide donor and human bone marrow stromal cells enhances angiogenesis and neurogenesis. *Brain Res*. 2004; 1005(1–2):21–28. [PubMed: 15044060]
32. Zhang RL, Zhang ZG, Zhang L, Chopp M. Proliferation and differentiation of progenitor cells in the cortex and the subventricular zone in the adult rat after focal cerebral ischemia. *Neuroscience*. 2001; 105(1):33–41. [PubMed: 11483298]
33. Xiong Y, Mahmood A, Meng Y, Zhang Y, Zhang ZG, Morris DC, Chopp M. Treatment of traumatic brain injury with thymosin beta in rats. *J Neurosurg*. 2011; 114(1):102–115. [PubMed: 20486893]
34. Lu D, Qu C, Goussev A, Jiang H, Lu C, Schallert T, Mahmood A, Chen J, Li Y, Chopp M. Statins increase neurogenesis in the dentate gyrus, reduce delayed neuronal death in the hippocampal CA3 region, and improve spatial learning in rat after traumatic brain injury. *J Neurotrauma*. 2007; 24(7):1132–1146. [PubMed: 17610353]
35. Zhang R, Wang Y, Zhang L, Zhang Z, Tsang W, Lu M, Zhang L, Chopp M. Sildenafil (Viagra) induces neurogenesis and promotes functional recovery after stroke in rats. *Stroke*. 2002; 33(11): 2675–2680. [PubMed: 12411660]
36. Lin B, Ginsberg MD, Zhao W, Alonso OF, Belayev L, Busto R. Quantitative analysis of microvascular alterations in traumatic brain injury by endothelial barrier antigen immunohistochemistry. *J Neurotrauma*. 2001; 18(4):389–397. [PubMed: 11336440]
37. Morris DC, Chopp M, Zhang L, Lu M, Zhang ZG. Thymosin beta4 improves functional neurological outcome in a rat model of embolic stroke. *Neuroscience*. 2010; 169(2):674–682. [PubMed: 20627173]
38. Li L, Jiang Q, Zhang L, Ding G, Gang Zhang Z, Li Q, Ewing JR, Lu M, Panda S, Ledbetter KA, Whitton PA, Chopp M. Angiogenesis and improved cerebral blood flow in the ischemic boundary area detected by MRI after administration of sildenafil to rats with embolic stroke. *Brain Res*. 2007; 1132(1):185–192. [PubMed: 17188664]
39. Clausen F, Lewen A, Marklund N, Olsson Y, McArthur DL, Hillered L. Correlation of hippocampal morphological changes and morris water maze performance after cortical contusion injury in rats. *Neurosurgery*. 2005; 57(1):154–163. discussion 154–163. [PubMed: 15987551]

40. Liu Z, Li Y, Zhang RL, Cui Y, Chopp M. Bone marrow stromal cells promote skilled motor recovery and enhance contralesional axonal connections after ischemic stroke in adult mice. *Stroke*. 2011; 42(3):740–744. [PubMed: 21307396]
41. Liu Z, Zhang RL, Li Y, Cui Y, Chopp M. Remodeling of the corticospinal innervation and spontaneous behavioral recovery after ischemic stroke in adult mice. *Stroke*. 2009; 40(7):2546–2551. [PubMed: 19478220]
42. Meng Y, Xiong Y, Mahmood A, Zhang Y, Qu C, Chopp M. Dose-dependent neurorestorative effects of delayed treatment of traumatic brain injury with recombinant human erythropoietin in rats. *J Neurosurg*. 2011; 115(3):550–560. [PubMed: 21495821]
43. Xiong Y, Mahmood A, Qu C, Kazmi H, Zhang ZG, Noguchi CT, Schallert T, Chopp M. Erythropoietin improves histological and functional outcomes after traumatic brain injury in mice in the absence of the neural erythropoietin receptor. *J Neurotrauma*. 2010; 27(1):205–215. [PubMed: 19715391]
44. Tsai PT, Ohab JJ, Kertesz N, Groszer M, Matter C, Gao J, Liu X, Wu H, Carmichael ST. A critical role of erythropoietin receptor in neurogenesis and post-stroke recovery. *J Neurosci*. 2006; 26(4):1269–1274. [PubMed: 16436614]
45. Grasso G, Graziano F, Sfacteria A, Carletti F, Meli F, Maugeri R, Passalacqua M, Certo F, Fazio M, Buemi M, Iacopino DG. Neuroprotective effect of erythropoietin and darbepoetin alfa after experimental intracerebral hemorrhage. *Neurosurgery*. 2009; 65(4):763–769. discussion 769–770. [PubMed: 19834382]
46. Grasso G, Sfacteria A, Meli F, Fodale V, Buemi M, Iacopino DG. Neuroprotection by erythropoietin administration after experimental traumatic brain injury. *Brain Res*. 2007; 1182:99–105. [PubMed: 17935704]
47. Cherian L, Goodman JC, Robertson C. Neuroprotection with erythropoietin administration following controlled cortical impact injury in rats. *J Pharmacol Exp Ther*. 2007; 322(2):789–794. [PubMed: 17470644]
48. Zhang Y, Xiong Y, Mahmood A, Meng Y, Qu C, Schallert T, Chopp M. Therapeutic effects of erythropoietin on histological and functional outcomes following traumatic brain injury in rats are independent of hematocrit. *Brain Res*. 2009; 1294:153–164. [PubMed: 19646970]
49. Rabie T, Marti HH. Brain protection by erythropoietin: a manifold task. *Physiology (Bethesda)*. 2008; 23:263–274. [PubMed: 18927202]
50. Leist M, Ghezzi P, Grasso G, Bianchi R, Villa P, Fratelli M, Savino C, Bianchi M, Nielsen J, Gerwien J, Kallunki P, Larsen AK, Helboe L, Christensen S, Pedersen LO, Nielsen M, Torup L, Sager T, Sfacteria A, Erbayraktar S, Erbayraktar Z, Gokmen N, Yilmaz O, Cerami-Hand C, Xie QW, Coleman T, Cerami A, Brines M. Derivatives of erythropoietin that are tissue protective but not erythropoietic. *Science*. 2004; 305(5681):239–242. [PubMed: 15247477]
51. Xiong Y, Mahmood A, Zhang Y, Meng Y, Zhang ZG, Qu C, Sager TN, Chopp M. Effects of posttraumatic carbamylated erythropoietin therapy on reducing lesion volume and hippocampal cell loss, enhancing angiogenesis and neurogenesis, and improving functional outcome in rats following traumatic brain injury. *J Neurosurg*. 2011; 114(2):549–559. [PubMed: 21073254]
52. Wang L, Zhang ZG, Gregg SR, Zhang RL, Jiao Z, LeTourneau Y, Liu X, Feng Y, Gerwien J, Torup L, Leist M, Noguchi CT, Chen ZY, Chopp M. The Sonic hedgehog pathway mediates carbamylated erythropoietin-enhanced proliferation and differentiation of adult neural progenitor cells. *J Biol Chem*. 2007; 282(44):32462–32470. [PubMed: 17804404]
53. Wang Y, Zhang ZG, Rhodes K, Renzi M, Zhang RL, Kapke A, Lu M, Pool C, Heavner G, Chopp M. Post-ischemic treatment with erythropoietin or carbamylated erythropoietin reduces infarction and improves neurological outcome in a rat model of focal cerebral ischemia. *Br J Pharmacol*. 2007; 151(8):1377–1384. [PubMed: 17603558]
54. Brines M, Grasso G, Fiordaliso F, Sfacteria A, Ghezzi P, Fratelli M, Latini R, Xie QW, Smart J, Su-Rick CJ, Pobre E, Diaz D, Gomez D, Hand C, Coleman T, Cerami A. Erythropoietin mediates tissue protection through an erythropoietin and common beta-subunit heteroreceptor. *Proc Natl Acad Sci U S A*. 2004; 101(41):14907–14912. [PubMed: 15456912]
55. Dore-Duffy P, Wang X, Mehedi A, Kreipke CW, Rafols JA. Differential expression of capillary VEGF isoforms following traumatic brain injury. *Neurol Res*. 2007; 29(4):395–403. [PubMed: 17626736]

56. Skold MK, von Gertten C, Sandberg-Nordqvist AC, Mathiesen T, Holmin S. VEGF and VEGF receptor expression after experimental brain contusion in rat. *J Neurotrauma*. 2005; 22(3):353–367. [PubMed: 15785231]
57. Wu H, Lu D, Jiang H, Xiong Y, Qu C, Li B, Mahmood A, Zhou D, Chopp M. Simvastatin-mediated upregulation of VEGF and BDNF, activation of the PI3K/Akt pathway, and increase of neurogenesis are associated with therapeutic improvement after traumatic brain injury. *J Neurotrauma*. 2008; 25(2):130–139. [PubMed: 18260796]
58. Lu KT, Sun CL, Wo PY, Yen HH, Tang TH, Ng MC, Huang ML, Yang YL. Hippocampal neurogenesis after traumatic brain injury is mediated by vascular endothelial growth factor receptor-2 and the Raf/MEK/ERK cascade. *J Neurotrauma*. 2011; 28(3):441–450. [PubMed: 21091268]
59. Lee C, Agoston DV. Inhibition of VEGF receptor 2 increased cell death of dentate hilar neurons after traumatic brain injury. *Exp Neurol*. 2009; 220(2):400–403. [PubMed: 19733172]
60. Skold MK, Risling M, Holmin S. Inhibition of vascular endothelial growth factor receptor 2 activity in experimental brain contusions aggravates injury outcome and leads to early increased neuronal and glial degeneration. *Eur J Neurosci*. 2006; 23(1):21–34. [PubMed: 16420412]
61. Lee C, Agoston DV. Vascular endothelial growth factor is involved in mediating increased de novo hippocampal neurogenesis in response to traumatic brain injury. *J Neurotrauma*. 2010; 27(3):541–553. [PubMed: 20001687]
62. Thau-Zuchman O, Shohami E, Alexandrovich AG, Leker RR. Vascular endothelial growth factor increases neurogenesis after traumatic brain injury. *J Cereb Blood Flow Metab*. 2010; 30(5):1008–1016. [PubMed: 20068579]
63. Greenberg DA, Jin K. From angiogenesis to neuropathology. *Nature*. 2005; 438(7070):954–959. [PubMed: 16355213]
64. Chopp M, Zhang ZG, Jiang Q. Neurogenesis, angiogenesis, and MRI indices of functional recovery from stroke. *Stroke*. 2007; 38(2 Suppl):827–831. [PubMed: 17261747]
65. Chen J, Chopp M. Neurorestorative treatment of stroke: cell and pharmacological approaches. *NeuroRx*. 2006; 3(4):466–473. [PubMed: 17012060]
66. Xiong Y, Mahmood A, Chopp M. Angiogenesis, neurogenesis and brain recovery of function following injury. *Curr Opin Investig Drugs*. 2010; 11(3):298–308.
67. Arai K, Jin G, Navaratna D, Lo EH. Brain angiogenesis in developmental and pathological processes: neurovascular injury and angiogenic recovery after stroke. *FEBS J*. 2009; 276(17):4644–4652. [PubMed: 19664070]
68. Beck H, Plate KH. Angiogenesis after cerebral ischemia. *Acta Neuropathol*. 2009; 117(5):481–496. [PubMed: 19142647]
69. Hansen TM, Moss AJ, Brindle NP. Vascular endothelial growth factor and angiopoietins in neurovascular regeneration and protection following stroke. *Curr Neurovasc Res*. 2008; 5(4):236–245. [PubMed: 18991658]
70. Madri JA. Modeling the neurovascular niche: implications for recovery from CNS injury. *J Physiol Pharmacol*. 2009; 60(Suppl 4):95–104. [PubMed: 20083857]
71. Xiong Y, Mahmood A, Chopp M. Neurorestorative treatments for traumatic brain injury. *Discov Med*. 2010; 10(54):434–442. [PubMed: 21122475]
72. Iwai M, Cao G, Yin W, Stetler RA, Liu J, Chen J. Erythropoietin promotes neuronal replacement through revascularization and neurogenesis after neonatal hypoxia/ischemia in rats. *Stroke*. 2007; 38(10):2795–2803. [PubMed: 17702962]
73. Wang L, Chopp M, Gregg SR, Zhang RL, Teng H, Jiang A, Feng Y, Zhang ZG. Neural progenitor cells treated with EPO induce angiogenesis through the production of VEGF. *J Cereb Blood Flow Metab*. 2008; 28(7):1361–1368. [PubMed: 18414495]
74. Byts N, Siren AL. Erythropoietin: a multimodal neuroprotective agent. *Exp Transl Stroke Med*. 2009; 1:4. [PubMed: 20142991]
75. Itokawa T, Nokihara H, Nishioka Y, Sone S, Iwamoto Y, Yamada Y, Cherrington J, McMahon G, Shibuya M, Kuwano M, Ono M. Antiangiogenic effect by SU5416 is partly attributable to inhibition of Flt-1 receptor signaling. *Mol Cancer Ther*. 2002; 1(5):295–302. [PubMed: 12489845]

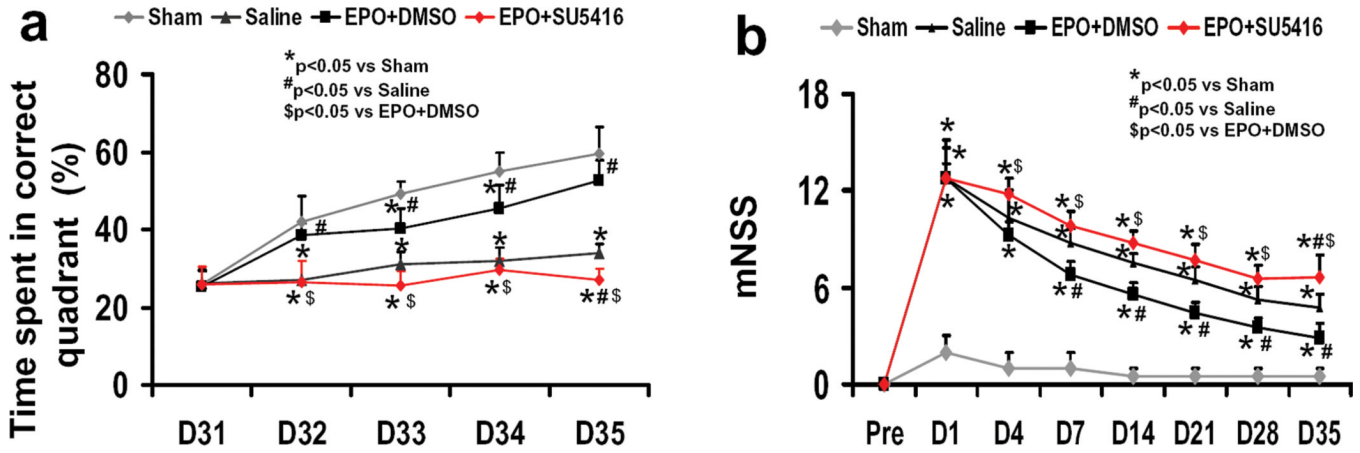


Fig. 1. The effect of EPO and SU5416 treatment on functional outcomes. (a) Spatial learning measured by a recent version of the Morris water maze test at days 31–35 after TBI. TBI significantly impaired spatial learning at days 32–35 compared to sham controls ($P<0.05$). Delayed treatment with EPO improves spatial learning performance at days 32–35 compared with the saline group ($P<0.05$). However, the spatial learning performance at days 32–35 in the EPO+SU5416 group is worse than that in the EPO+DMSO group ($P<0.05$). (b) The plot shows the functional improvement detected on the modified neurological severity scores (mNSS). EPO treatment significantly lowers mNSS at days 4–35 compared to saline group ($P<0.05$). However, the functional recovery (mNSS) at days 4–35 in the EPO+SU5416 group is worse than that in the EPO+DMSO group ($P<0.05$). Data represent mean \pm SD. * $P<0.05$ vs. Sham group. # $P<0.05$ vs. Saline group. \$ $P<0.05$ vs. EPO+DMSO. n (rats/group) = 8.

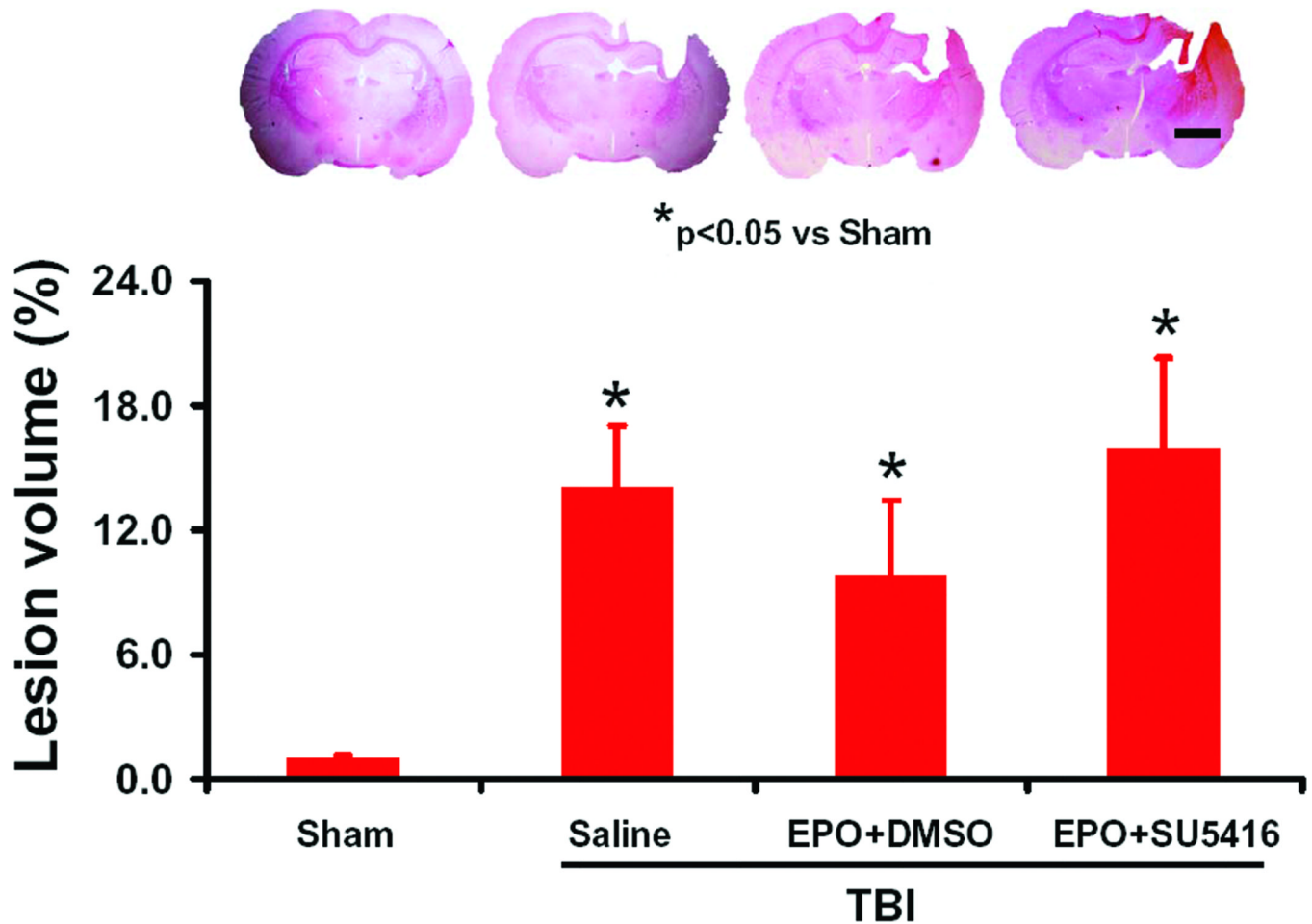


Fig. 2.

Effect of EPO and SU5416 on lesion volume examined at 35 days after TBI. TBI caused a significant cortical lesion compared to sham controls (H&E staining). Delayed treatment with EPO combined with DMSO had a tendency to reduce lesion volume without a significance compared to the saline group ($P < 0.05$). EPO+SU5416 treatment had a tendency to increase the lesion volume but did not reach a significant level compared to the EPO +DMSO group. Data represent mean \pm SD. Scale bar = 3 mm. * $P < 0.05$ vs. Sham group. n (rats/group) = 8.

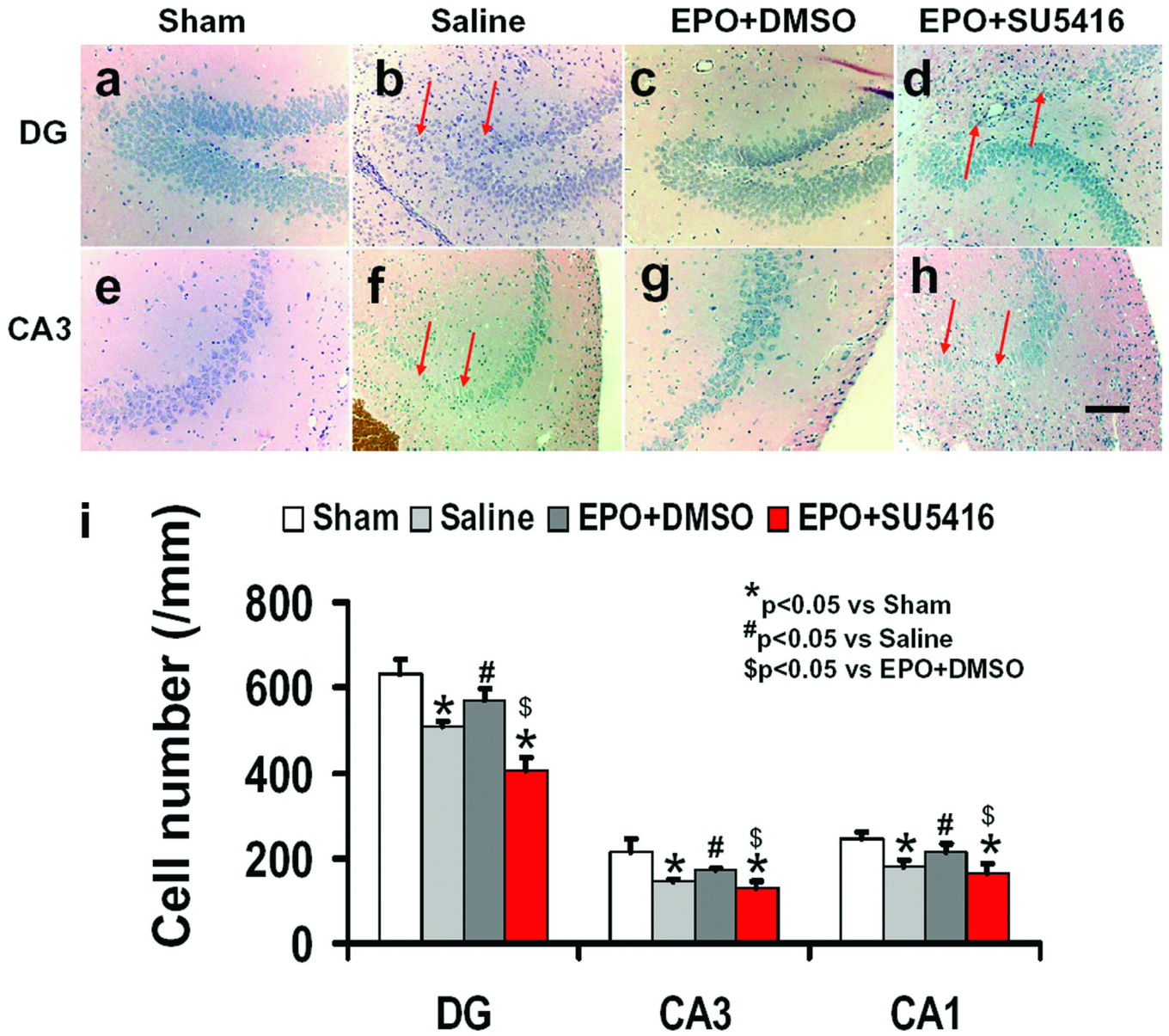


Fig. 3. Effect of EPO and SU5416 on cell loss in the ipsilateral hippocampus at 35 days after TBI. H&E staining: a-h. TBI caused significant cell loss in the dentate gyrus (DG), CA3 and CA1 regions (b, f, and i; $P<0.05$) of the ipsilateral hippocampus compared to sham controls (a and e). Arrows indicate cell loss. Delayed treatment with EPO (c, g, and i) significantly reduced cell loss as compared with the saline group ($P<0.05$). The cell number in the DG, CA3 and CA1 region is shown in (i). As compared to the EPO+DMSO group, the cell number in the EPO+SU5416 group was significantly decreased (d, h, and i; $P<0.05$). Data represent mean \pm SD. Scale bar = 50 μ m (a-h). * $P<0.05$ vs. Sham group. # $P<0.05$ vs. Saline group. \$ $P<0.05$ vs. EPO+DMSO. n (rats/group) = 8.

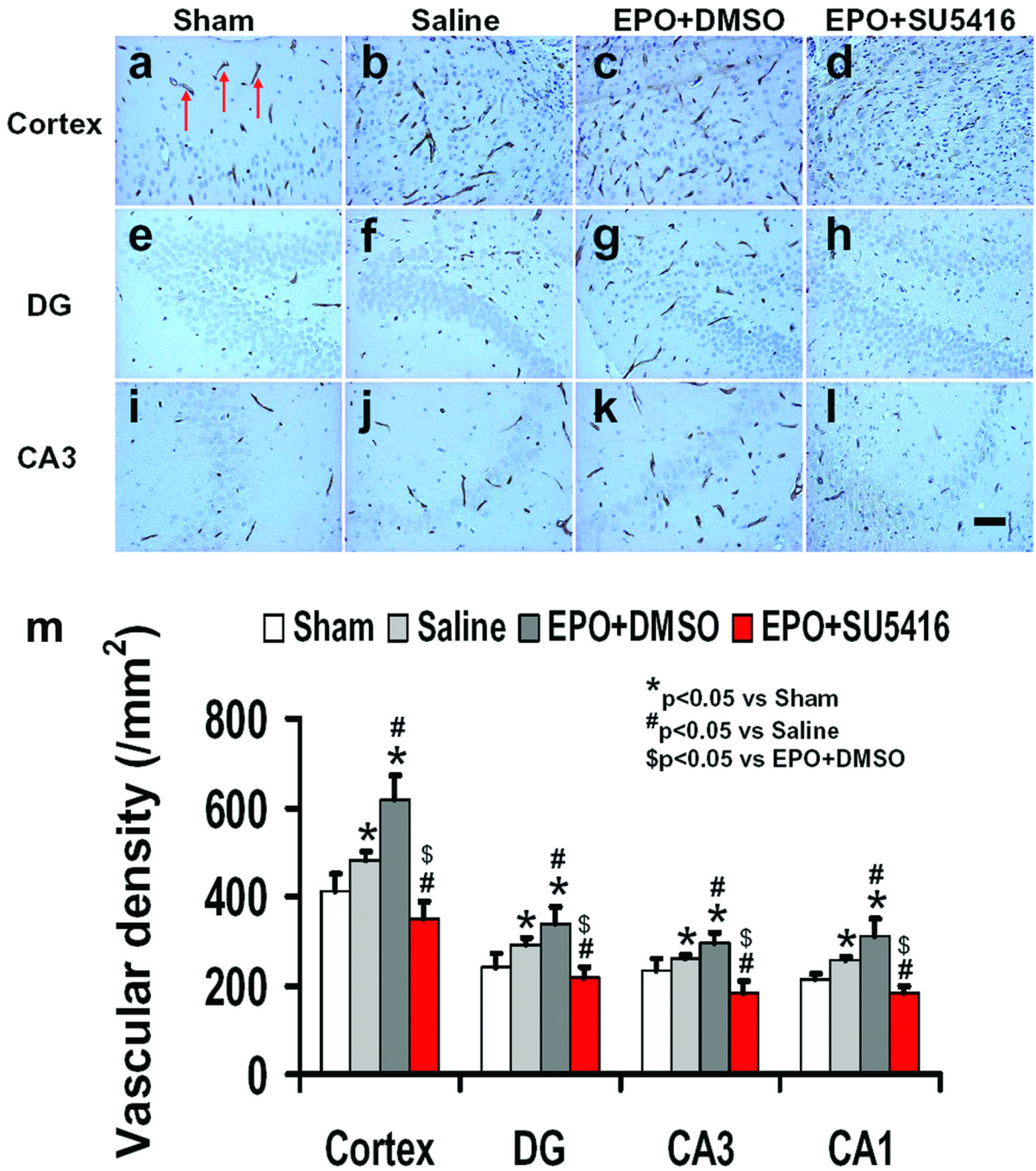


Fig. 4. Effect of EPO and SU5416 on EBA-staining vascular structure in the injured cortex, ipsilateral DG and CA3 region 35 days after TBI. Arrows in a (as an example) indicate EBA-positive vascular structure. TBI alone (b, f, and g; $P < 0.05$) significantly increased the vascular density in these regions compared to sham controls (a, e, and i; $P < 0.05$). EPO treatment further enhanced angiogenesis after TBI compared to saline groups (c, g and k; $P < 0.05$). As compared to the EPO+DMSO group, the EPO+SU5416 group had a significantly decreased vascular density in these regions (d, h, and i; $P < 0.05$). The density of EBA-stained vasculature is shown in (m). Data represent mean \pm SD. Scale bar = 25 μ m (i).

* $P < 0.05$ vs. Sham group. # $P < 0.05$ vs. Saline group. \$ $P < 0.05$ vs. EPO+DMSO. n (rats/group) = 8.

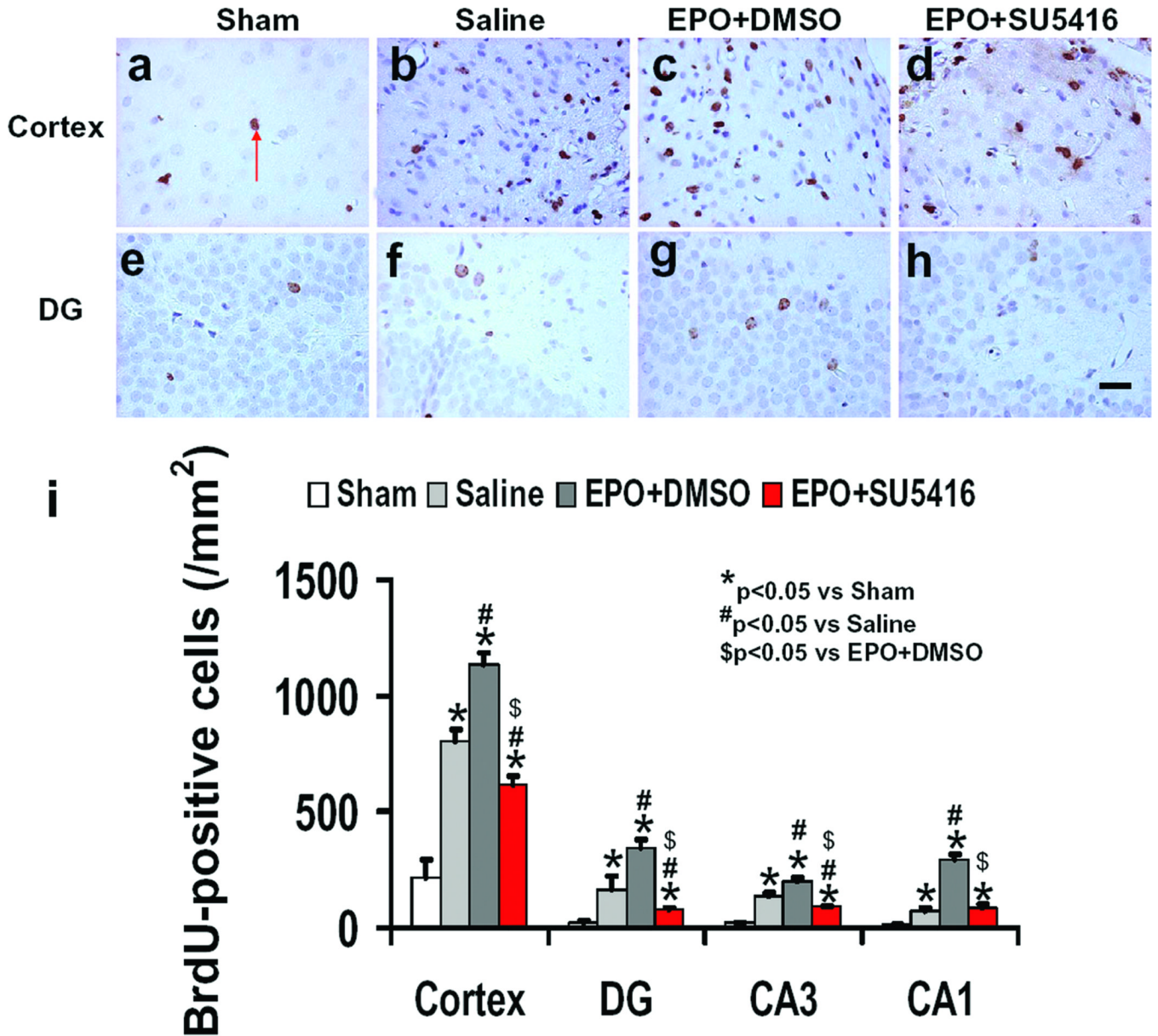


Fig. 5. Effect of EPO and SU5416 on cell proliferation in the injured cortex and ipsilateral DG 35 days after TBI. The cells with BrdU (brown stained) that clearly localized to the nucleus (hematoxylin stained) were counted as BrdU-positive cells (arrow in a as an example). TBI alone (b and f) significantly increased the number of BrdU-positive cells in the ipsilateral cortex and DG compared to sham controls (a and e; $P<0.05$). The number of BrdU-positive cells is shown in i. EPO treatment significantly increased the number of BrdU-positive cells in these regions (c and g; $P<0.05$) compared to the saline group. As compared to the EPO +DMSO group, the EPO+SU5416 group had a significantly smaller number of BrdU-positive cells in these regions (d and h; $P<0.05$). Data represent mean \pm SD. Scale bar = 25 μ m. * $P<0.05$ vs. Sham group. # $P<0.05$ vs. Saline group. \$ $P<0.05$ vs. EPO+DMSO. n (rats/group) = 8.

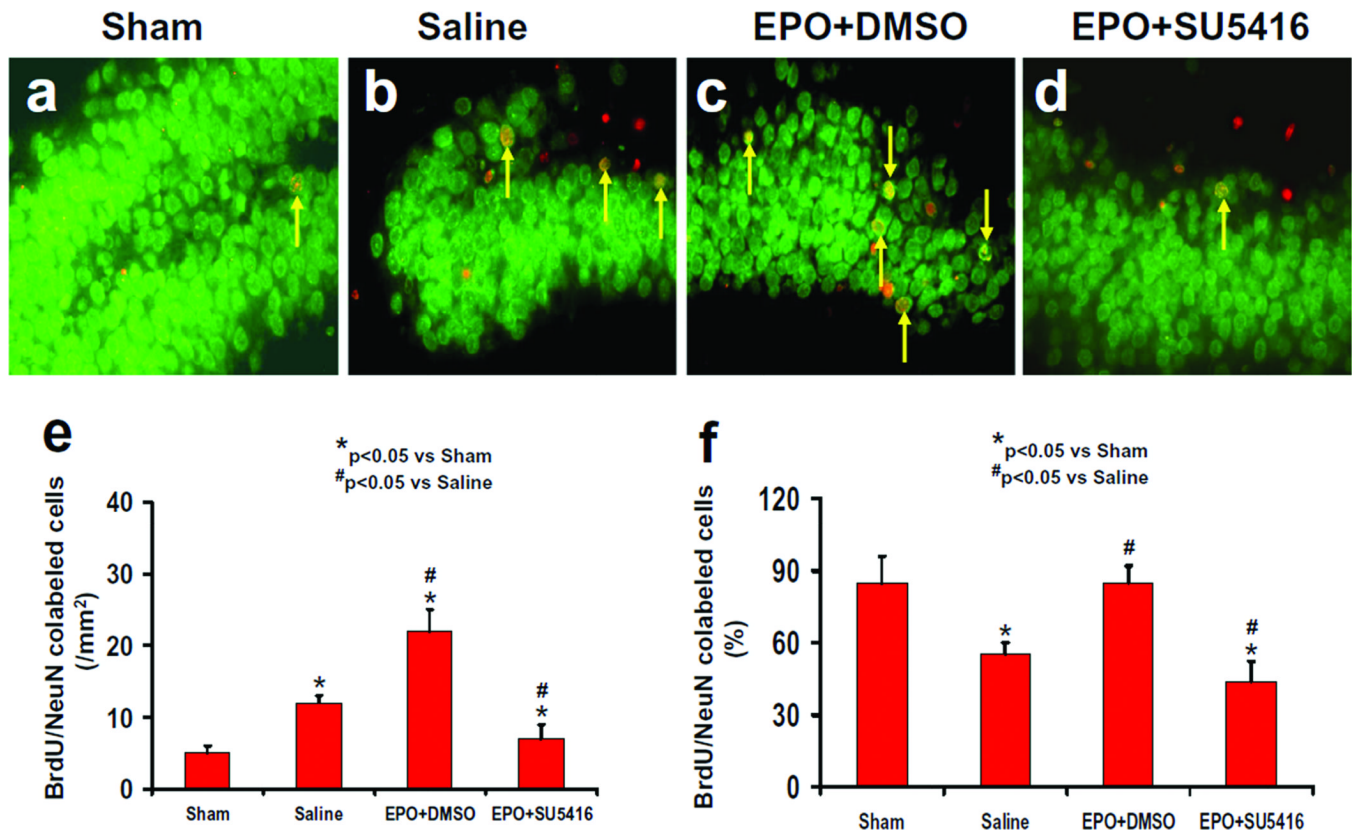


Fig.6. Effect of EPO and SU5416 on NeuN/BrdU-positive cells in the ipsilateral DG 35 days after TBI. Double fluorescent staining for BrdU (red) and NeuN (green) to identify newborn neurons (yellow after merge, as arrows indicate) in the ipsilateral DG. TBI significantly increased the newborn neuron number in the injured DG (b) compared to sham (a; $P < 0.05$). EPO treatment significantly increased the number of NeuN/BrdU-positive cells (c; $P < 0.05$) compared to the saline group. As compared to the EPO+DMSO group, the EPO+SU5416 group had a significantly smaller number of NeuN/BrdU-positive cells (d; $P < 0.05$). The bar graphs show the number (e) and the percentage (f) of newborn neurons in the DG. The number of newborn neurons (NeuN/BrdU-colocalized cells) was counted in the DG and expressed per mm². The percentage of newborn neurons was the ratio of the number of NeuN/BrdU-positive cells to the total number of BrdU-positive cells in the DG. Data represent mean \pm SD. * $P < 0.05$ vs. Sham group. # $P < 0.05$ vs. Saline group. n (rats/group) = 8.

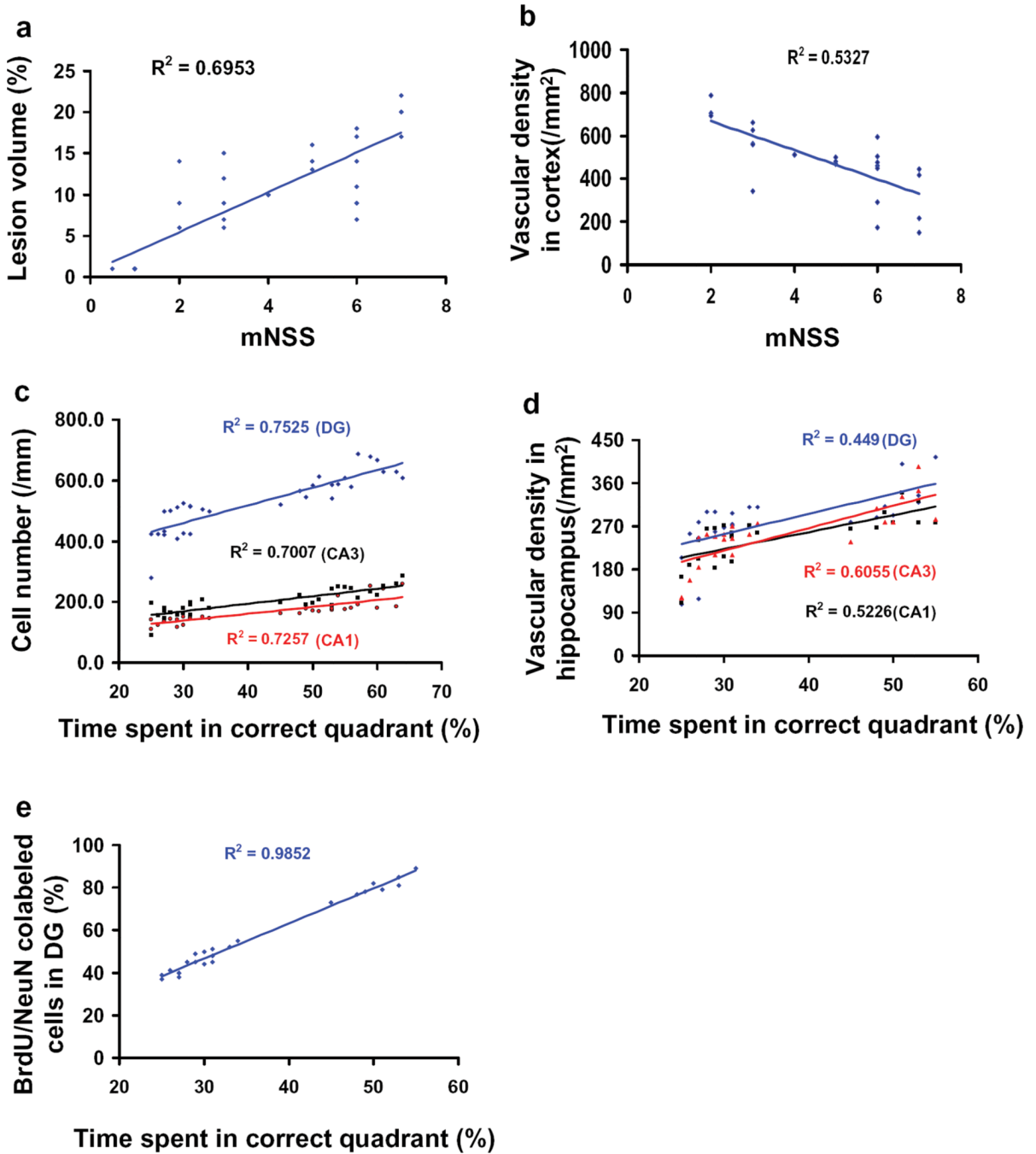


Fig. 7. Correlation of functional outcomes with lesion volume, cell loss, angiogenesis, and neurogenesis. Data from all four groups were included to generate the correlations between functional and histological outcomes. The top panel line graphs show that the functional outcomes (mNSS scores) are significantly and positively correlated with the lesion volume (a; $P < 0.05$) but inversely correlated with the vascular density (b; $P < 0.05$). The other panel line graphs show that spatial learning performance is significantly and positively correlated with the number of neuron cells (c), vascular density (d), and NeuN/BrdU-positive cells (e) in the ipsilateral hippocampus measured at day 35 in rats after TBI and EPO treatment ($P < 0.05$). Data represent mean \pm SD. n (rats/group) = 8.

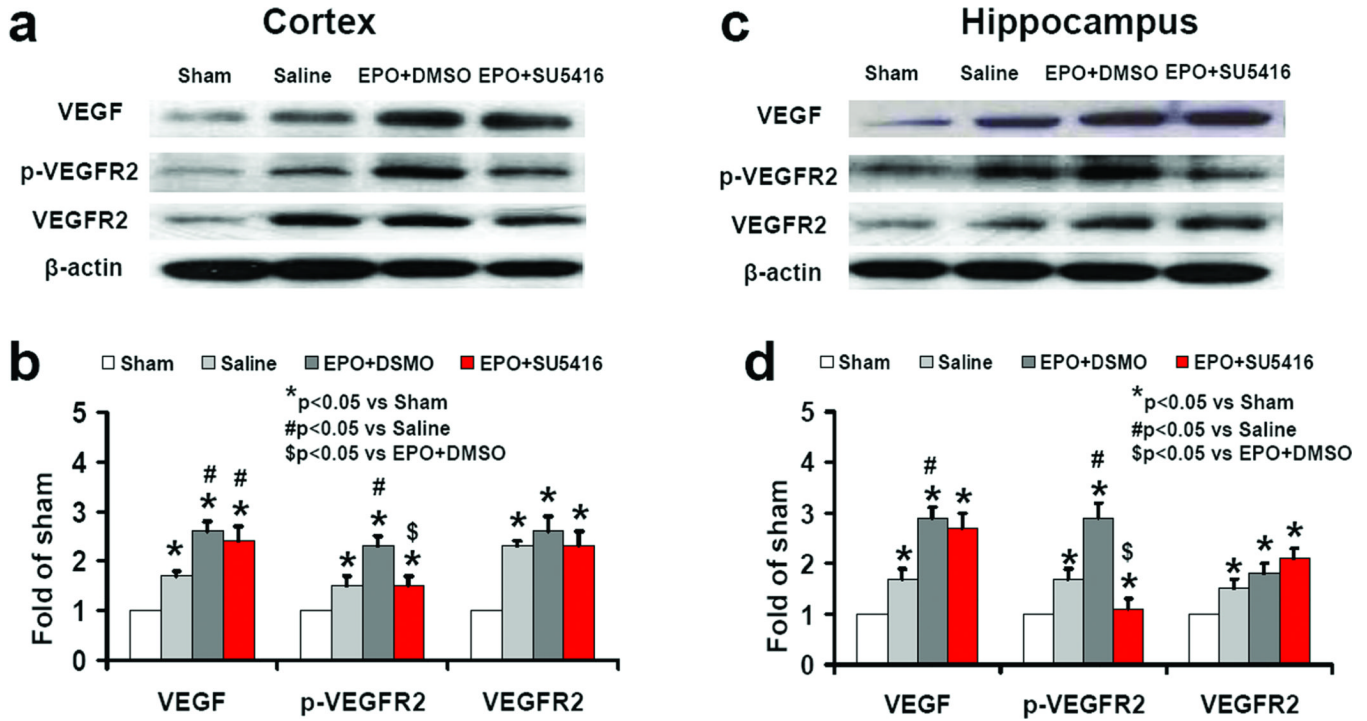


Fig. 8. Effect of EPO and SU5416 on VEGF and VEGFR2 level in the brain after TBI. Western blot analyses show the effects of EPO and SU5416 on VEGF and phosphorylation of VEGFR2 in brain tissue after TBI (a and c). Bar graphs show the quantitative data of protein band density (b and d). TBI significantly increased VEGF level and p-VEGFR2 in the injury boundary zone (a) and hippocampus (c) compared to sham (a and e; $P<0.05$). EPO treatment significantly increased the VEGF expression and p-VEGFR2 ($P<0.05$) compared to the saline group. As compared to the EPO+DMSO group, the EPO+SU5416 group did not significantly affect the VEGF level in the brain (c and d; $P>0.05$); SU5416 significantly decreased the p-VEGFR2 level in the brain ($P<0.05$). The bar graphs (i) show the density of VEGF-positive astrocytes. Data represent mean \pm SD. * $P<0.05$ vs. Sham group. # $P<0.05$ vs. Saline group. \$ $P<0.05$ vs. EPO+DMSO. n (rats/group) = 4.

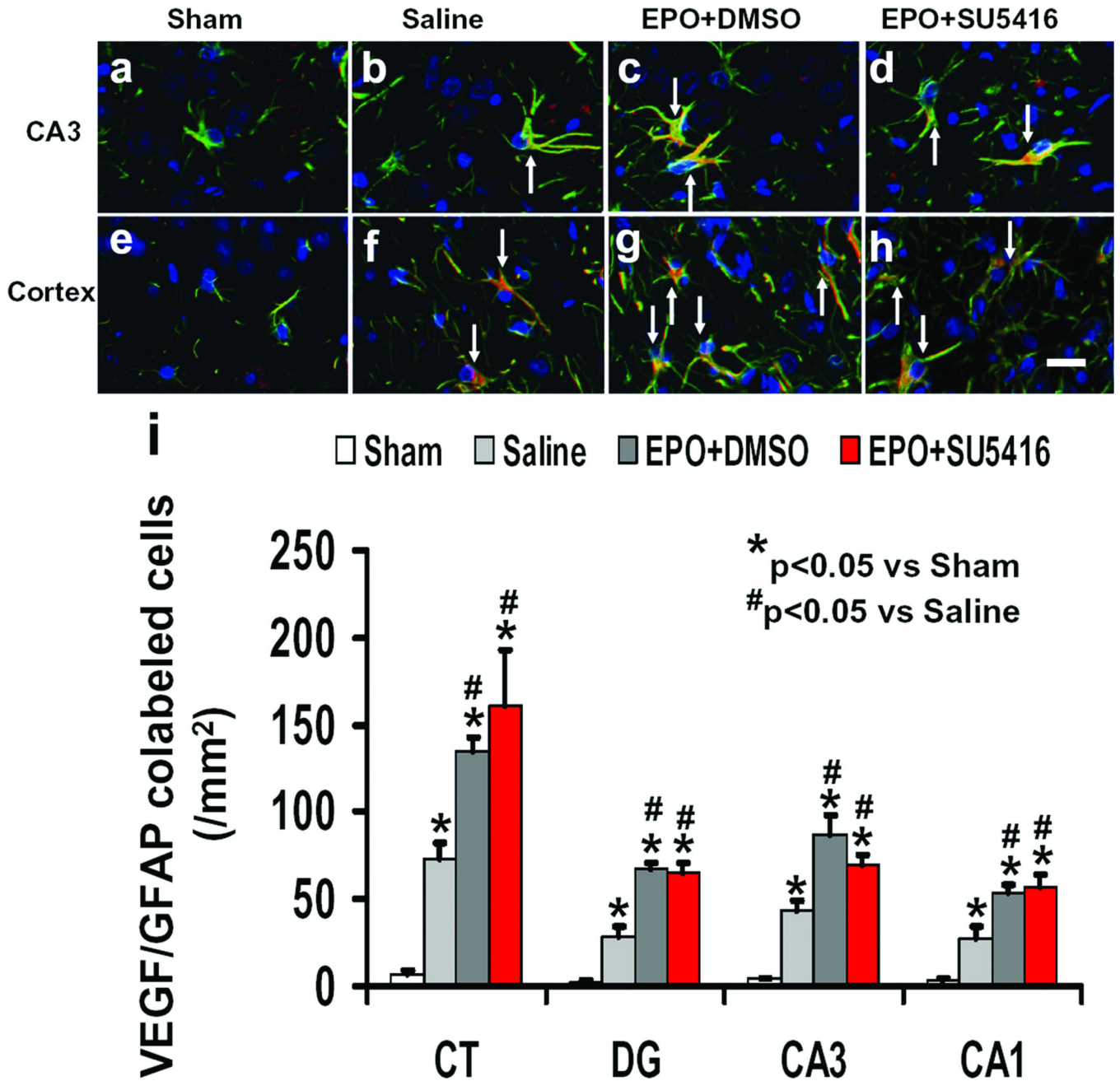


Fig. 9. Effect of EPO and SU5416 on VEGF expression in astrocytes after TBI. Triple fluorescent staining for VEGF (red), GFAP (green) and DAPI (blue) to identify VEGF-positive astrocytes (yellow after merge, as arrows indicate). TBI significantly increased the number of VEGF-positive astrocytes in the hippocampal CA3 region (b) and injury boundary zone (f) compared to sham (a and e; $P < 0.05$). EPO treatment significantly increased the number of VEGF-positive astrocytes (c and g; $P < 0.05$) compared to the saline group. As compared to the EPO+DMSO group, the EPO+SU5416 group did not significantly affect the number of VEGF-positive astrocytes (d and h; $P > 0.05$). The bar graphs (i) show the density of VEGF-positive astrocytes. Data represent mean \pm SD. Scale bar = 25 μ m (d). * $P < 0.05$ vs. Sham group. # $P < 0.05$ vs. Saline group. n (rats/group) = 4.